Applied Catalysis B: Environmental 90 (2009) 307–312

Contents lists available at ScienceDirect

Applied Catalysis B: Environmental

journal homepage: www.elsevier.com/locate/apcatb

Catalytic performance of manganese cobalt oxides on methane combustion at low temperature

Junhua Li *, Xi Liang, Shicheng Xu, Jiming Hao

Department of Environmental Science and Engineering, Tsinghua University, Beijing, 100084, PR China

ARTICLE INFO

Article history:
Received 9 December 2008
Received in revised form 19 March 2009
Accepted 21 March 2009
Available online 31 March 2009

Keywords:
Methane combustion
Cobalt
Manganese
Spinel
Promotional effect
Crystal defections

ABSTRACT

Manganese cobalt oxides with different Co/Mn ratios have been prepared by co-precipitation methods, and their catalytic performance on methane combustion were evaluated from 250 °C to 400 °C at a space velocity of 36,000 h^{-1}. A significant improvement of activity was observed over Co5Mn1 catalysts with a Co/Mn molar ratio of 5:1, and the catalytic activity reached 90% of methane conversion at 320 °C. Oxygen mobility – reflected by the appearance of O_2^- – was probably a key factor that influenced the oxidation rate of methane below 320 °C. The doping of manganese into the spinel structure of cobalt oxide increased crystal defections, which probably caused the increase of the amount of octahedrally coordinated divalent cobalt cations that are responsible for catalytic activity. The hydroxyl groups observed on the manganese-doped catalysts would also explain the promotional effects.

1. Introduction

With the soaring gasoline prices and the increasingly strict emission limits, compressed natural gas (CNG) engines are widely applied to vehicles nowadays. Compared to conventional gasoline and diesel engines, it has much lower emissions of nitrogen oxides and toxic hydrocarbons. Moreover, the relative abundant storage of natural gas makes CNG more attractive. However, the main component of natural gas is methane which is a type of greenhouse gas, and it has 72 times (over 20 years) the global warming potential (GWP) of CO_2 [1]. Therefore, the abatement of unconverted methane exhausted from CNG vehicles at low temperature (temperature of exhausted gas from lean burn CNG seldom exceeding 500 °C) [2] becomes rather important.

Catalytic combustion of methane (CCM) is a promising technology that can convert methane into carbon dioxide at relatively low temperature, and is extensively studied over the last decade. Noble metal-based catalysts, especially Pd-based ones [3–7] can exhibit outstanding catalytic behavior at low temperatures. Nevertheless, catalysts based on transition metals, such as Mn, Cu, Cr, Fe, Co, In [8,9] become appealing due to lower cost and relative abundant resources.

Among all the transition metal oxides, Co_3O_4 is believed to be a good CCM candidate. Xiao et al. [10] reported cobalt oxides on different supports and found ZrO_2 supported catalyst have the highest activity compared to TiO_2, Al_2O_3, MgO supported catalysts and bulk Co_3O_4. Liotta et al. [11,12] studied Co_3O_4/CeO_2 and Co_3O_4/CeO_2–ZrO_2 containing 30 wt.% of Co_3O_4 and found ceria and ceria–zirconia helps to disperse the active phase Co_3O_4 and promotes the reduction at low temperature. Zavyalova et al. [13] found various nanosized Co_3O_4/γ-Al_2O_3 catalysts prepared by a combination of wetness impregnation to have defective structures and exhibit high activity in the total oxidation of methane. On the other hand, platinum and manganese oxide catalysts [14,15] have been applied in methane combustion. High activity of methane oxidation has also been observed on Mn-doped ZrO_2 [16] by Choudhary et al. Li et al. [17] have studied the CCM activities of Co/Mn mixed oxide catalysts prepared by sol–gel methods. Although the promoting effects of water vapor were discovered on the Co/Mn mixed oxide catalysts, no promoting effects of manganese to the catalytic activity were found.

In this work, a series of Co/Mn mixed catalysts were prepared by co-precipitation method, and the promotional effect of manganese on cobalt oxides was investigated. The sample with a Co/Mn ratio of 5:1 exhibited rather high catalytic activity, reaching 90% conversion at approximately 320 °C. Several char-

* Corresponding author at: Department of Environmental Science and Engineering, Tsinghua University, Beijing, 100084, PR China. Tel.: +86 10 62782030.
E-mail address: lijunhua@tsinghua.edu.cn (J. Li).

0926-3373/$ – see front matter © 2009 Elsevier B.V. All rights reserved.
doi:10.1016/j.apcatb.2009.03.027

acterization methods were applied to study the textural properties of the prepared samples, and the diffuse reflectance infrared Fourier transform spectroscopy (DRIFTS) analyses could also deepen our understanding of the promotional effect and reaction mechanism.

2. Experimental

2.1. Catalyst preparation

The Co/Mn mixed oxide catalysts were prepared by a co-precipitation method. Stoichiometric amounts of $Co(NO_3)_2{\cdot}6H_2O$, $Mn(CH_3COO)_2{\cdot}4H_2O$ were first dissolved in deionized water, then the precursors were mixed according to stoichiometric amounts and dripped slowly into an ammonium bicarbonate solution. After the precipitates were aged with stirring at room temperature for 8 h, they were filtered and washed with 80 mL ethanol and deionized water until the pH reached 7.0. The powders were dried at room temperature overnight. Dried at 90 °C for 6 h, the samples were then calcined at 400 °C for 4 h to obtain crystalline composite oxides. Catalysts were identified as Co_xMn_y, x and y are based on the Co and Mn mole content, for example, Co5Mn1 represents the catalyst of which the Co:Mn (mol) is 5:1. Pure Co_3O_4 and MnO_x, marked respectively as Co10Mn0 and Co0Mn10, were also prepared by the similar procedures described above.

2.2. Catalytic activity measurement

The methane combustion activities of all the oxide catalysts were tested in a fixed-bed quartz reactor (i.d. 8 mm) containing 0.5 g catalysts, at the temperature range of 250–400 °C. Operating conditions were as follows: 1 vol.% CH_4, 10 vol.% O_2 and N_2 as the balance gas, with a total flow rate of 150 mL/min, corresponding to a WHSV about 36,000 mL h^{-1} g^{-1}. The concentration of CH_4 in inlet and outlet gases was measured by an on-line gas chromatograph (Shimadzu GC 17A). The activities were evaluated in terms of CH_4 conversion defined as $(C_{in} - C_{out})/C_{in} \times 100\%$, C_{in} and C_{out} being methane concentration corresponding to the inlet and outlet, respectively. Activity data were collected at every measurement points after stabilizing for 20 min.

2.3. Catalyst characterization

X-ray diffraction (XRD) measurements were carried out with a Bruker D8-Advance diffractometer using Ni filtered Cu Kα radiation. The applied current and voltage were 40 mA and 40 kV, respectively. During the analysis, the samples were scanned from 10° to 90° at a speed of 4°/min.

BET-surface area was measured by N_2 adsorption at liquid nitrogen temperature using a NOVA4000 automated gas sorption system.

The X-ray photoelectron spectra (XPS) chemical analyzing was carried out on a PHI Quantera SXM system. Al Kα radiation was used as the source and the C 1s peak was used as a reference.

The in-situ DRIFT was carried out on Nicolet Fourier Infrared Spectrum with diffuse reflection situ pool and high delicacy MCT detector. The DRIFT spectra during methane combustion experiment were recorded with a Nicolet Nexus spectrometer equipped with a liquid nitrogen-cooled MCT detector, collecting 100 scans at a spectral resolution of 4 cm^{-1}. Prior to each experiment, samples were oxidized in a flow of 10 vol.% O_2 at 400 °C for 60 min. The reactions in the cell were performed under a flow of 20 mL/min gas mixture containing methane and oxygen with N_2 as balance gas.

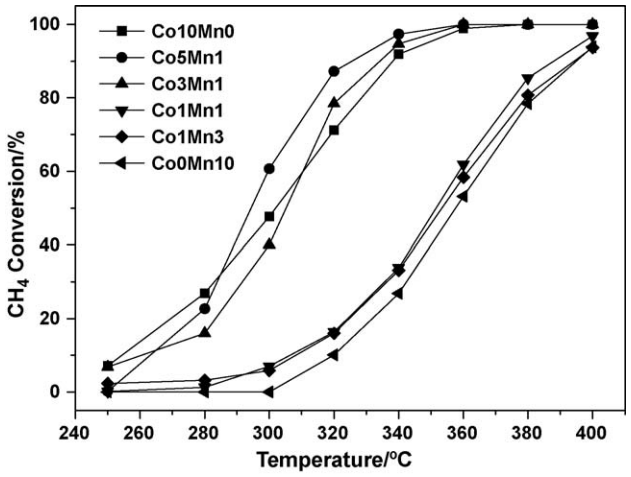

Fig. 1. The catalytic activities of Co_xMn_y for methane combustion as the function of temperature. Gas mixture: 1% CH_4, 10% O_2, N_2 as balance gas. WHSV = 36,000 mL h^{-1} g^{-1}.

3. Results and discussion

3.1. Catalytic combustion of methane

Fig. 1 shows the methane combustion activities of Co/Mn catalysts. According to the results, the catalysts could be divided into two types. The first type of catalysts had Co/Mn molar ratio above 3. These catalysts exhibited relatively high activities in methane combustion. At 340 °C, their CH_4 conversions were all above 90%. Especially for Co5Mn1 catalyst, it showed the best activity, reaching 90% methane conversion at the temperature of 320 °C. Below 300 °C, the activity of Co10Mn0 was a little higher than that of others. Nevertheless, compared to other catalysts in this category, its activity rose slowly with the increase of temperature, reaching only about 70% even at 320 °C.

On the other hand, as can be seen clearly from the figure, catalysts with Co/Mn molar ratio equal or less than 1 are less effective than the others. In summary, if T_{90} (the temperature needed to reach 90% CH_4 conversion) was set as the standard of activity, the descending order of activity for all the observed catalysts was as follows: Co5Mn1 > Co3Mn1 > Co10Mn0 > > Co1Mn1 > Co1Mn3 ≈ Co0Mn10.

3.2. Catalyst characterization

3.2.1. BET results

Table 1 lists the BET surface area of all the prepared catalysts. Pure cobalt oxide (Co10Mn0) had a surface area of 62.6 m^2/g, which was much smaller than that of pure manganese oxide whose surface area reached 183.9 m^2/g. It can be seen from the table that, except for Co3Mn1, surface areas of Mn-doped catalysts increased with the increment of manganese contents. Since no substantial differences in surface areas was observed in catalysts containing both Mn and Co relating to catalytic activity, for these catalysts,

Table 1
BET surface areas and catalytic activities of $Co_xMn_yO_z$ catalysts.

Sample	Surface area (m^2/g)	T_{20} (°C)	T_{50} (°C)	T_{90} (°C)
Co10Mn0	62.55	265	297	339
Co5Mn1	147.65	280	293	324
Co3Mn1	158.46	282	306	333
Co1Mn1	150.25	323	350	386
Co1Mn3	154.49	323	351	392
Co0Mn10	183.94	331	358	393

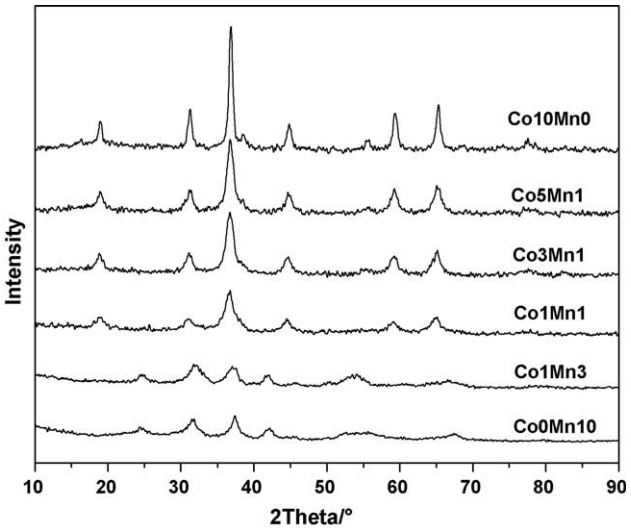

Fig. 2. X-ray diffraction patterns of Co_xMn_y with various molar ratios of Co and Mn.

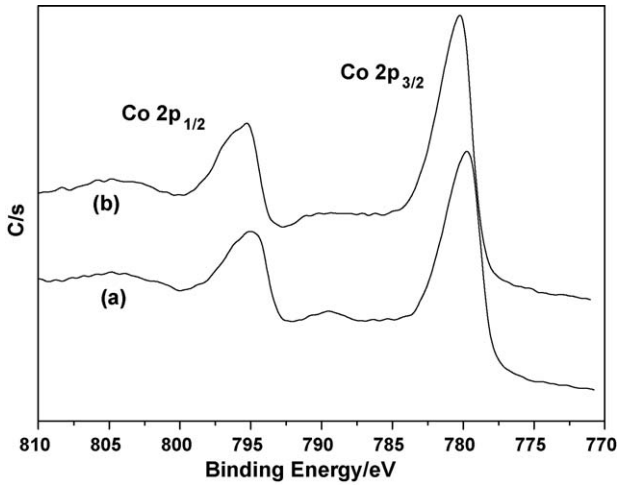

Fig. 3. XPS multiplex spectra of cobalt peaks in Co_xMn_y samples: (a) Co10Mn0; (b) Co5Mn1.

surface areas have not significant influence on their catalytic performances.

3.2.2. XRD results

The XRD patterns of Co_xMn_y are shown in Fig. 2. According to the results, the observed samples could be divided to two types. Falling to the first type, catalysts (Co10Mn0, Co5Mn1 and Co3Mn1) with above or equal 50% cobalt content all belonged to the cube spinel structure of pure Co_3O_4, and there was no CoO phase in the bulk. Peak intensity decreased and band width at half maximum enlarged with the increase of manganese content, and the maximum peak intensity was observed on Co10Mn0, this indicates that Co10Mn0 has a larger average size of crystallites than those of cobalt–manganese oxides and manganese oxide. These results also prove the lowest specific surface area of Co10Mn0 due to the well crystallite. Besides, it is possible that the number of crystal defection increases in smaller crystallites as the amount of doped-manganese increased. Although manganese was introduced to Co_3O_4 up to 50%, no phase corresponding to Mn_2O_3 was observed obviously, which implied the well-dispersion of Mn into the lattice of Co_3O_4, and that also excluded conglomeration of MnO_x. The XRD patterns of the second type of catalysts (Co1Mn1, Co1Mn3 and Co0Mn10) – with more than 50% manganese content – resembled to that of Mn_2O_3 [17]. Locations and the intensities of the XRD peaks of Co1Mn1, Co1Mn3 and Co0Mn10 were almost the same. Coincidentally, samples categorized into the first type exhibited better activity than those assigned to the second type. Respectful amounts of lattice imperfection observed in Co5Mn1 and Co3Mn1 were responsible for their enhanced catalytic activities, which will be demonstrated in the following parts.

3.2.3. XPS results

XPS results survey of Co_xMn_y samples are listed in Table 2. As has to be clarified here, since the patterns of O 1s binding energy were asymmetrical, we split the peaks into two, attributing them to different O species [18]. The resolution procedure for the O 1s peak used two Gaussian functions each of variable position, width, and intensity. O_I represented the peak indicating higher binding energy, and O_{II} represented the lower one. The high binding energy of O_I was due to absorption of oxygen species at the surface [19,20] while low binding energy of O_{II} could be ascribed to lattice oxygen [21,22]. Area ratio of O_I/O_{II} could be a yardstick to measure the proportion of the two different oxygen species, thus higher area ratio indicates larger amount of vacant oxygen. It can be seen from the table that Co5Mn1 had comparatively lower amount of surface oxygen than Co10Mn0 and Co0Mn10, and the fewest vacant oxygen.

Fig. 3 shows the XPS pattern of cobalt on the surface of Co10Mn0 and Co5Mn1. Binding energy of Co $2p_{3/2}$ in Co10Mn0 peaked at 779.8 eV, which confirmed its chemical component of Co_3O_4 [23]. A slight increase of Co $2p_{3/2}$ binding energy in Co5Mn1 was observed. Binding energy for Mn^{2+} and Mn^{4+} are almost the same in lots of manganese oxides [24], here we employed ΔE3s [25] to identify the valence of manganese. Higher value of ΔE3s indicates lower oxidative state of manganese. The XPS spectra of Mn 3s in Co0Mn10 and Co5Mn1 are shown in Fig. 4. Since the Mn content was rather low in Co5Mn1, the intensities of the peaks were quite weak and ambiguous. On the smoothed pattern, for Co0Mn10, binding energy of Mn $3s_{3/2}$ and that of Mn $3s_{1/2}$ were 83.8 eV and 89.3 eV; and for Co5Mn1, the values were 83.7 eV and 89.4 eV respectfully. For Co0Mn10, ΔE3s = 89.3 − 83.8 eV = 5.5 eV; that is to say the valence of manganese in Co0Mn10 was +2.8 [25]. For Co5Mn1, ΔE3s = 89.4 − 83.7 eV = 5.7 eV, hence the overall valence of manganese in Co5Mn1 was approximately +2.5 [25].

Cations in spinel are located in two different sites: tetrahedral sites and octahedral sites. In the normal distribution of spinel, divalent ions are located on the tetrahedral sites (A sites), while trivalent ones on the octahedral sites (B sites). In the inverse distribution, the situation is the opposite [26–28]. Most spinels have a partially inversed structures, and both divalent and

Table 2
XPS Results of $Co_xMn_yO_z$ with various ratios of Co and Mn.

Sample	Surface atomic composition (%)					Peak position (eV)				Area ratios O_I/O_{II}
	Co	Mn	O	Co $2p_{1/2}$	Co $2p_{3/2}$	Mn $2p_{1/2}$	Mn$2p_{3/2}$	O_I	O_{II}	
Co10Mn0	29.8	–	70.2	794.9	779.8	–	–	531.7	529.7	1.67
Co5Mn1	34.7	7.0	58.3	795.2	780.1	654.0	641.9	531.3	530.3	1.31
Co0Mn10	–	28.9	71.1	–	–	653.6	642.0	531.6	529.7	1.79

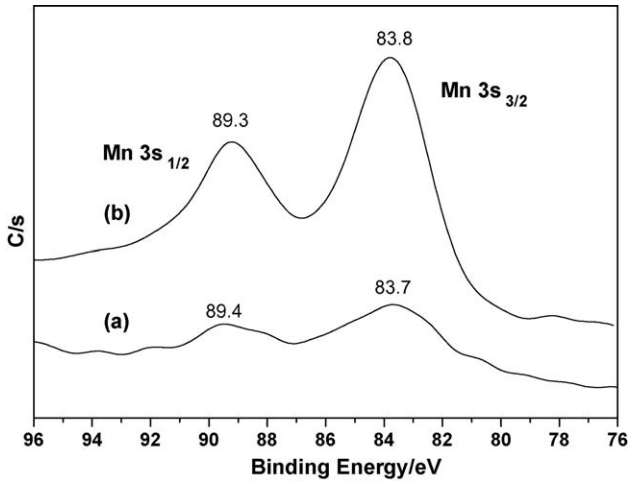

Fig. 4. XPS multiplex spectra of manganese peaks in Co_xMn_y samples: (a) Co5Mn1; (b) Co0Mn10.

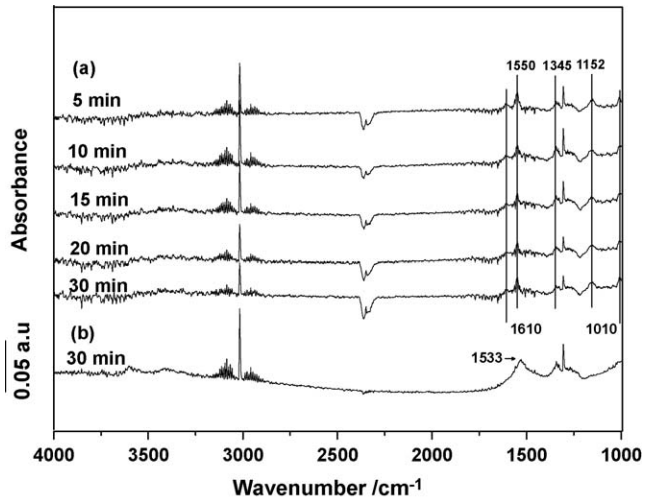

Fig. 5. IR Spectra of Co5Mn1 after adsorption of (a) 1% CH_4 and 10% O_2, (b) 1% CH_4 at 250 °C.

trivalent cobalt cations exist in Co_3O_4 (Co10Mn0). With respect of Co5Mn1, according to the XRD patterns, the doped-Mn ions probably took the place of cobalt ions in its solid solution-like phase. Since its overall valence of manganese was about +2.5; both trivalent and divalent manganese cations existed in the spinel structure. The following equilibrium would be struck among cobalt and manganese ions.

$$Mn_{octa}^{3+} + Co_{tetra}^{2+} \rightleftarrows Mn_{tetra}^{3+} + Co_{octa}^{2+} \rightleftarrows Mn_{tetra}^{2+} + Co_{octa}^{3+}$$

The balance between these cations would be determined by their structural and redox properties. First, to consider the spinel structures, trivalent cobalt cation has very strong crystal field stabilization energy in B sites [27], and that is why most of them coordinate octahedrally in Co_3O_4. Though crystal field stabilization energy of trivalent manganese cation is higher; if locates at B site, it will give rise to a local tetragonal distortion of the crystal due to Jahn–Teller effect [26]. In addition, divalent manganese is prior to divalent cobalt in their competition for A site [26]. Therefore, the octahedrally coordinated manganese is not stable, and adjacent cobalt cations would tend to be converted from divalent to trivalent. On the contrary, considering the redox property of the two elements, it implies that divalent cobalt could not be easily oxidized by trivalent manganese. Therefore, the discordance of the oxidative states and textural properties of these two elements would lead to the partially disorder of the spinel structure, which would influence the catalytic property of Co5Mn1.

3.3. DRIFTS studies

3.3.1. Active oxygen species

The DRIFTS spectra of co adsorption of methane and oxygen on Co5Mn1 at 250 °C are presented in Fig. 5a, and they were taken in the flow of 1% methane and 10% oxygen (N_2 as balance). Bands at 3016 cm^{-1}, 1610 cm^{-1}, 1550 cm^{-1}, 1345 cm^{-1}, 1304 cm^{-1} and 1152 cm^{-1} were found. Bands rose at 3016 cm^{-1} and 1304 cm^{-1} are due to C–H bonds in methane [29]. The bands at 1550 cm^{-1} and 1345 cm^{-1} could be attributed to carbonate [29,30], most likely in monodentate form; and bands at 1610 cm^{-1} to hydroxyl group. According to literature [31], the O_2^- bands formed by the absorbed O_2 ranges from 1050 cm^{-1} to 1200 cm^{-1}, therefore, 1152.2 cm^{-1} band could be ascribed to O_2^-.

The adsorption of methane was studied by flowing 1% methane in the absence of oxygen (see Fig. 5b). The bands at 1533 cm^{-1} and 1345 cm^{-1} corresponded to carbonate. However, bands at 1152 cm^{-1} were not as significant as that observed in the presence of oxygen. This showed that methane could be oxidized by surface oxygen atoms, and the formation of O_2^- was due to the interactions between surface active sites and gaseous oxygen.

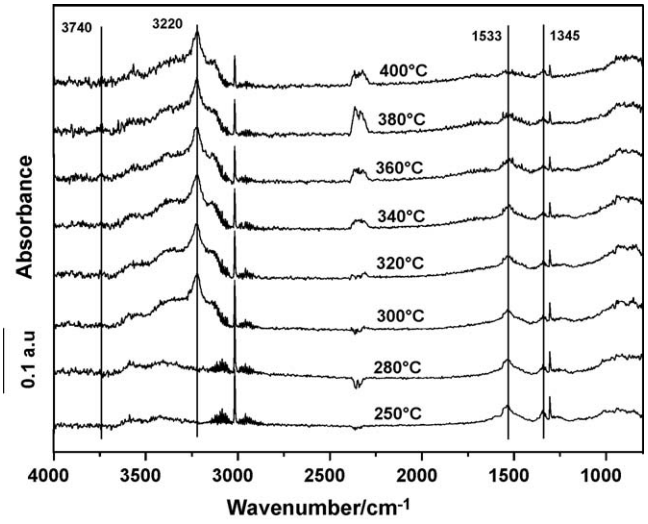

Fig. 6. IR Spectra of methane combustion on Co5Mn1 as function of temperature (1% CH_4 and 10% O_2).

The spectra of the combustion reactions are shown in Fig. 6. The spectra were recorded under a flow of 1% methane and 10% oxygen (N_2 as balance) for 30 min after the cell reached the desired temperature. As has been demonstrated in the previous parts, the catalytic activity increased with the raise of temperature. On the spectra, signals of CO_2 (2350 cm^{-1}) increased as temperature raised while that of carbonates flattened. No peaks at 2000 cm^{-1} (carbon monoxide [32]) were found. Above 250° C, bands raised by O_2^- vanished, they might be quickly consumed by the hydrocarbons, or they were not the crucial intermediate at relatively higher temperature. Moreover, the bands at 3220 cm^{-1} and 3740 cm^{-1} were observed above 300° C.

Catalytic activity of spinel depends mainly on octahedral sites exposed on the surface [28,33], and the abnormal divalent cobalt located in octahedral sites [34,35] could be the active site on cobalt oxides. Since divalent cobalt favors tetrahedral sites, it is probably through this different preference, they can react with the absorbed oxygen to form trivalent cobalt and O_2^-. Other than Co5Mn1, O_2^-

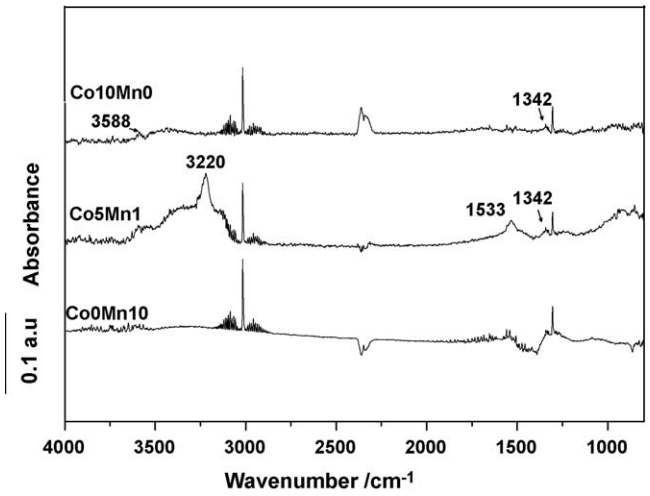

Fig. 7. IR Spectra of methane combustion on (a) Co10Mn0, (b) Co5Mn1, (c) Co0Mn10 at 300 °C (1% CH_4 and 10% O_2).

was also detected on Co10Mn0 below 300 °C. Given the fact that Co10Mn0 and Co5Mn1 exhibited better catalytic performance than catalysts belonging to the other groups below 300 °C (as shown in Fig. 1), oxygen mobility – reflected by the appearance of O_2^- – was probably a key factor that influenced the oxidation rate of methane under this temperature range.

3.3.2. Hydroxyl groups

Fig. 7 compares the DRIFTS spectra of Co5Mn1, Mn_2O_3 and Co_3O_4 in methane combustion, and the spectra were taken 30 min after the temperature of the cell reached 300 °C. For Co5Mn1 and Co10Mn0, besides the difference shown at the IR range of 1700–1300 cm^{-1} that the band of carbonate was more noticeable on Co5Mn1 than on Co10Mn0, another major difference appeared at the IR range of 3700–3100 cm^{-1}. On Co10Mn0 the board but weak band starting from 3250 cm^{-1} to 3650 cm^{-1} with the tiny peak at 3588 cm^{-1} indicated the existence of hydroxyl species [36–38], mainly multiply coordinated ones [37]. On Co5Mn1, within the same range, the comparative small band at 3740 cm^{-1} could be assigned to terminal hydroxyl species [37]; and the huge band peaked at 3220 cm^{-1} was a sign of hydroxyls bond to dopant trivalent cations [39]. Moreover, a broad band peaked at around 1000 cm^{-1} on Co5Mn1 indicated the formation of hydroxyl on MnO(OH) [40]. On the spectrum of Mn_2O_3, neither carbonates nor hydroxyl were detected.

Above 300 °C, better catalytic activity was observed on Co5Mn1. The combustion of methane should be completed through at least two steps: methane oxidation and dehydroxylation. The first step has to do with the oxygen mobility of the catalysts. However, since Co10Mn0 took advantages over Co5Mn1 on oxygen mobility, that may not be responsible to the promotional effects. While hydroxyl groups that were observed on Co5Mn1 might have to do with the promotion in catalytic performance, with respect to dehydroxylation, which should be completed by exchange of proton between surface hydroxyls and absorbed oxygen. Promoting effects of water vapor have also been found in cobalt/manganese mixed oxides [17]. In the lattice of normal spinel, one of the two adjacent cations occupies a tetrahedral vacancy, and the other locates in an octahedral one. Tetrahedrally coordinated manganese might adhere to an octahedrally coordinated cobalt, and share three oxygen atoms with it. Thus, hydroxyls attached on octahedrally coordinated cobalt could possibly transfer its proton to the nearby oxygen bonding to manganese. As the manganese ion becomes trivalent while locate at a tetrahedral site, the formed MnO(OH) would be rather unstable; and it would react with oxygen (gaseous or adsorbed) to form a MnO_6 octahedron, which would finally be distorted or reduced by the nearby divalent cobalt to form a much stable MnO_4 tetrahedron with a tetrahedrally coordinated divalent manganese cation. If the above-mentioned proton exchange between CoO_x complex and the MnO_x complex completed faster than the dehydroxylation steps occurred among cobalt cations, this would possibly explain the promotional effects of manganese.

4. Conclusions

Manganese, as the dopant, can enhance the catalysts' activity in catalytic combustion of methane. Doped in an appropriate amount, manganese causes the disorders in the spinel structure of cobalt oxides; consequently, they would enhance the activity of the reactive ions in the octahedral sites and probably facilitate the dehydroxylation steps, and thus increase the catalytic performance of the Co/Mn mixed oxides.

Acknowledgments

The work was financially supported by National Natural Science Fund of China (Grant No. 20677034), and the National High-Tech Research and Development (863) Program of China (Grant No. 2006AA060301), and New Century Excellent Talents in University of China (NCET-2005-78).

References

[1] P. Forster, V. Ramaswamy, P. Artaxo, T. Berntsen, R. Betts, D.W. Fahey, J. Haywood, J. Lean, D.C. Lowe, G. Myhre, J. Nganga, R. Prinn, G. Raga, M. Schulz, R. Van Dorland, in: S. Solomon, D. Qin, M. Manning, Z. Chen, M. Marquis, K.B. Averyt, M. Tignor, H.L. Miller (Eds.), Climate Change 2007: The Physical Science Basis. Contribution of Working Group I to the Fourth Assessment Report of the Intergovernmental Panel on Climate Change, Cambridge University Press, Cambridge, United Kingdom and New York, NY, USA, 2007.
[2] D. Fino, N. Russo, G. Saracco, V. Specchia, Prog. Solid State Chem. 35 (2007) 501.
[3] R.J. Farrauto, M.C. Hobson, T. Kennelly, E.M. Waterman, Appl. Catal. A 81 (1992) 227.
[4] R.J. Farrauto, J.K. Lampert, M.C. Hobson, E.M. Waterman, Appl. Catal. B 6 (1995) 263.
[5] K.-I. Fujimoto, F.H. Ribeiro, M. Avalos-Borja, E. Iglesia, J. Catal. 179 (1998) 431.
[6] Y. Ozawa, Y. Tochihara, M. Nagai, S. Omi, Catal. Commun. 4 (2003) 87.
[7] Z. Li, G.B. Hoflund, J. Nat. Gas Chem. 12 (2003) 153.
[8] V.R. Choudhary, B.S. Uphade, S.G. Pataskar, A. Keshavaraja, Angew. Chem. Int. Ed. Engl. 35 (1996) 2393.
[9] J. Li, H. Fu, L. Fu, J. Hao, Environ. Sci. Technol. 40 (2006) 6455.
[10] T.-C. Xiao, S.-F. Ji, H.-T. Wang, K.S. Coleman, M.L.H. Green, J. Mol. Catal. A: Chem. 175 (2001) 111.
[11] L.F. Liotta, G. Di Carlo, G. Pantaleo, G. Deganello, Appl. Catal. B 70 (2007) 314.
[12] L.F. Liotta, G. Di Carlo, G. Pantaleo, G. Deganello, Catal. Commun. 6 (2005) 329.
[13] U. Zavyalova, P. Scholz, B. Ondruschka, Appl. Catal. A 323 (2007) 226.
[14] A. Barresi, S.L. Hung, L.D. Pfefferle, Chem. Eng. J. 50 (1992) 123.
[15] J. Carnö, M. Ferrandon, E. Björnbom, S. Järås, Appl. Catal. A 155 (1997) 265.
[16] V.R. Choudhary, B.S. Uphade, S.G. Pataskar, Appl. Catal. A 227 (2002) 29.
[17] W. Li, Y. Lin, Y. Zhang, Catal. Today 83 (2003) 239.
[18] J.P. Bonnelle, J. Grimblot, A. D'huysser, J. Electron. Spectrosc. Relat. Phenom. 7 (1975) 151.
[19] J.P. Holgado, G. Munuera, J.P. Espinos, A.R. Gonzalez-Elipe, Appl. Surf. Sci. 158 (2000) 164.
[20] F. Larachi, J. Pierre, A. Adnot, A. Bernis, Appl. Surf. Sci. 195 (2002) 236.
[21] A. Bensalem, F. Bozonverduraz, M. Delamar, G. Bugli, Appl. Catal. A 121 (1995) 81.
[22] S. Hamoudi, F. Larachi, A. Adnot, A. Sayari, J. Catal. 185 (1999) 333.
[23] L.F. Liotta, G. Di Carlo, G. Pantaleo, A.M. Venezia, G. Deganello, Appl. Catal. B 66 (2006) 217.
[24] M.L. Rojas, J.L.G. Fierro, L.G. Tejuca, A.T. Bell, J. Catal. 124 (1990) 41.
[25] V.R. Galakhov, M. Demeter, S. Bartkowski, M. Neumann, N.A. Ovechkina, E.Z. Kurmaev, N.I. Logachevskaya, Y.M. Mukovskii, J. Mitchell, D.L. Ederer, Phys. Rev. B: Condens. Matter 65 (2002) 113102.
[26] F.A. Kroger, The Chemistry of Imperfect Crystals, 1st ed., North-Holland Pub. Co., Amsterdam, 1964.
[27] T.A.S. Ferreira, J.C. Waerenborgh, M.H.R.M. Mendonca, M.R. Nunes, F.M. Costa, Solid. State Sci. 5 (2003) 383.
[28] E. Manova, T. Tsoncheva, C. Estournes, D. Paneva, K. Tenchev, I. Mitov, L. Petrov, Appl. Catal. A 300 (2006) 170.
[29] M. Schmal, M.M.V.M. Souza, V.V. Alegre, M.A.P. da Silva, D.V. Cesar, C.A.C. Perez, Catal. Today 118 (2006) 392.

[30] O. Demoulin, M. Navez, P. Ruiz, Appl. Catal. A 295 (2005) 59.
[31] Z. Li, G. Xu, G.B. Hoflund, Fuel Process. Technol. 84 (2003) 1.
[32] G. Lapisardi, L. Urfels, P. Gélin, M. Primet, A. Kaddouri, E. Garbowski, S. Toppi, E. Tena, Catal. Today 117 (2006) 564.
[33] D. Kaucký, A. Vondrová, J. Dedecek, B. Wichterlová, J. Catal. 194 (2000) 318.
[34] F.E. Trigueiro, C.M. Ferreira, J.-C. Volta, W.A. Gonzalez, P.G.P. de Oliveria, Catal. Today 118 (2006) 425.
[35] M.A. Ulla, R. Spretz, E. Lombardo, W. Daniell, H. Knözinger, Appl. Catal. B 29 (2001) 217.
[36] J.A. Dean, Lange's Handbook of Chemistry, 15th ed., McGraw-Hill, New York, 1999.
[37] D. Ciuparu, E. Perkins, L. Pfefferle, Appl. Catal. A 263 (2004) 145.
[38] K. Persson, L.D. Pfefferle, W. Schwartz, A. Ersson, S.G. Järås, Appl. Catal. B 74 (2007) 242.
[39] A.J. Berry, H.S.C. O'Neill, J. Hermann, D.R. Scott, Earth Planet. Sci. Lett. 261 (2007) 134.
[40] P. Aitchison, B. Ammundsen, J. Rozière, G.R. Burns, D.J. Jones, Solid State Ionics 176 (2005) 813.